Proceedings of the ASME 2010 3rd Joint US-European Fluids Engineering Summer Meeting and 8th International Conference on Nanochannels, Microchannels, and Minichannels
FEDSM-ICNMM2010
August 1-5, 2010, Montreal, Canada

FEDSM-ICNMM2010-30072

INTERACTION OF LIQUID PROPELLANT AND COUPLED SYSTEM STRUCTURE FOR ATLAS V LAUNCH VEHICLE

Kirk W. Dotson
The Aerospace Corporation
2350 E. El Segundo Blvd.
El Segundo, California, USA 90245

Brian H. Sako
The Aerospace Corporation
2350 E. El Segundo Blvd.
El Segundo, California, USA 90245

Daniel R. Morgenthaler
United Launch Alliance
12257 S. Wadsworth Blvd.
Littleton, Colorado, USA 80125

ABSTRACT

In structural modeling of launch vehicles, liquid propellant is sometimes rigidly attached to feedline walls. This assumption precludes the interaction of structural modes with propellant pressure and flow. An analysis of fluid-structure interaction (FSI) for the Atlas V launch vehicle revealed that structural models with rigidly-attached propellant yield unconservative response predictions under some conditions. In particular, during the maximum acceleration time of flight, pressure oscillations acting at bends in the Atlas V liquid oxygen (LO_2) feedline excite 15-20 Hz structural modes that have considerable gain on the feedline and at the spacecraft interface. The investigation also revealed that the venting of gas from the pogo accumulator is an excitation source and changes the dynamic characteristics of the hydraulic system. The FSI simulation produced during the investigation can be adapted to mission-specific conditions, such that responses and loads are conservatively predicted for any Atlas V flight.

Keywords: fluid-structure interaction, launch vehicles, feedlines, pogo accumulator, venting.

INTRODUCTION

Atlas V Launch Vehicle Overview

The first flight of the Atlas V launch vehicle is shown in Fig. 1. Figure 2 shows an exploded view of the 400 series configuration of the Atlas V. Launch events for a typical 400 series flight profile are defined in Fig. 3.

Fig 1. Launch of Atlas V 400 series [1].

Liquid propellants feed the boost engine of launch vehicles and flow through lines extending from tank outlets to the engine interface. Liquid oxygen (LO_2) and rocket propellant (RP-1) are used for the Atlas V boost stage [1]. As shown in Fig. 2, the LO_2 feedline runs from

the bottom of the LO_2 tank, along the outside of the RP-1 tank, to the RD-180 boost engine.

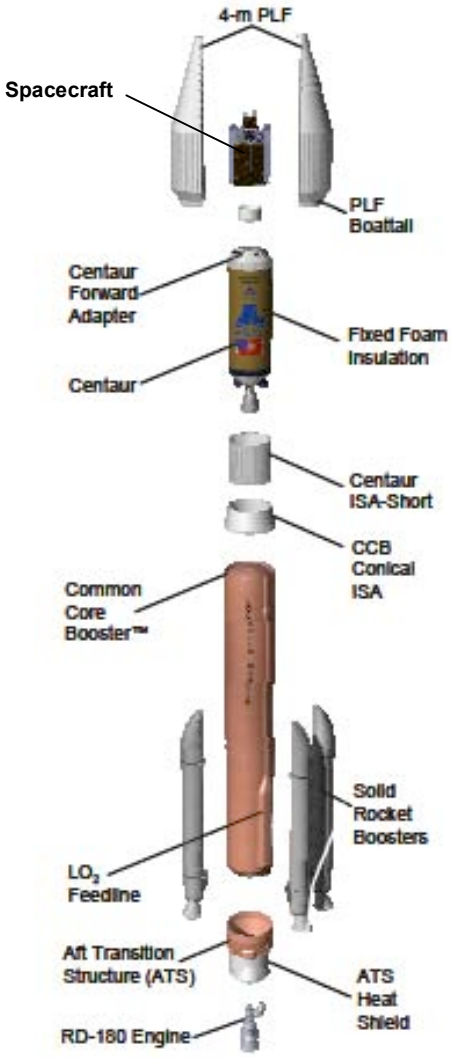

Fig 2. Atlas V 400 series launch system [1].

The maximum acceleration time of flight (Max G) for the Atlas V is identified in Fig. 3. Boost engine cutoff (BECO) occurs at the end of the Max G event. This paper addresses responses during Max G, and just prior to BECO, which are affected by fluid-structure interaction.

Pogo Mitigation Devices

The tanks, feed lines, and engine of launch vehicles vibrate during liftoff and ascent. This vibration causes the flow of the propellants in the feed lines and engine to oscillate, leading to thrust oscillation. The resulting thrust oscillation can cause the structure to vibrate even more, which increases the fluid oscillations, which causes greater vibration, and so on in a progressive feedback loop. This represents a system instability, and the resulting oscillations can become extreme [2].

Propellant oscillations in feedlines can interact with structural responses of the coupled launch vehicle-spacecraft system. Unstable feedback, called pogo, can lead to large system responses and catastrophic failure. This feedback is generally exacerbated when natural frequencies of axial modes of the launch vehicle structure coincide with natural frequencies of fluid in the feedlines.

Launch vehicles commonly use hardware devices called accumulators to prevent pogo. Accumulators add compliance to the hydraulic system, such that the fundamental fluid mode has a frequency that is well below those of the critical axial modes of the structure [3].

Several types of pogo accumulators are shown in Fig. 4. If enclosed gas provides the compliance of the pogo accumulator (as, for example in Fig. 4b), this gas is commonly vented prior to engine cutoff.

A pogo accumulator is used in the LO_2 feedline of the Atlas V launch vehicle. The accumulator is vented during the Max G time of flight.

Atlas V Flight Instrumentation

Atlas V flights are instrumented with accelerometers at the interface between the spacecraft and Centaur forward adapter (see Fig. 2). These measurements can be resolved into the launch vehicle axial and lateral (pitch and yaw) coordinates. Some Atlas V missions have also flown with accelerometers and pressure transducers mounted on the LO_2 feedline.

After every Atlas V flight, telemetry data are used to investigate the accuracy of response predictions. If significant discrepancies exist between flight data and preflight predictions, improvements in loads methodology are implemented before response analyses are conducted for subsequent missions.

Atlas V Flight Response at Max G

Telemetry data from several Atlas V flights indicate that 15-20 Hz structural responses tend to increase in amplitude during the Max G time of flight. The measured launch vehicle and spacecraft interface accelerations tend to maximize just prior to shutdown of the RD-180 boost engine and generally exceed in amplitude the 15-20 Hz responses at other times of flight.

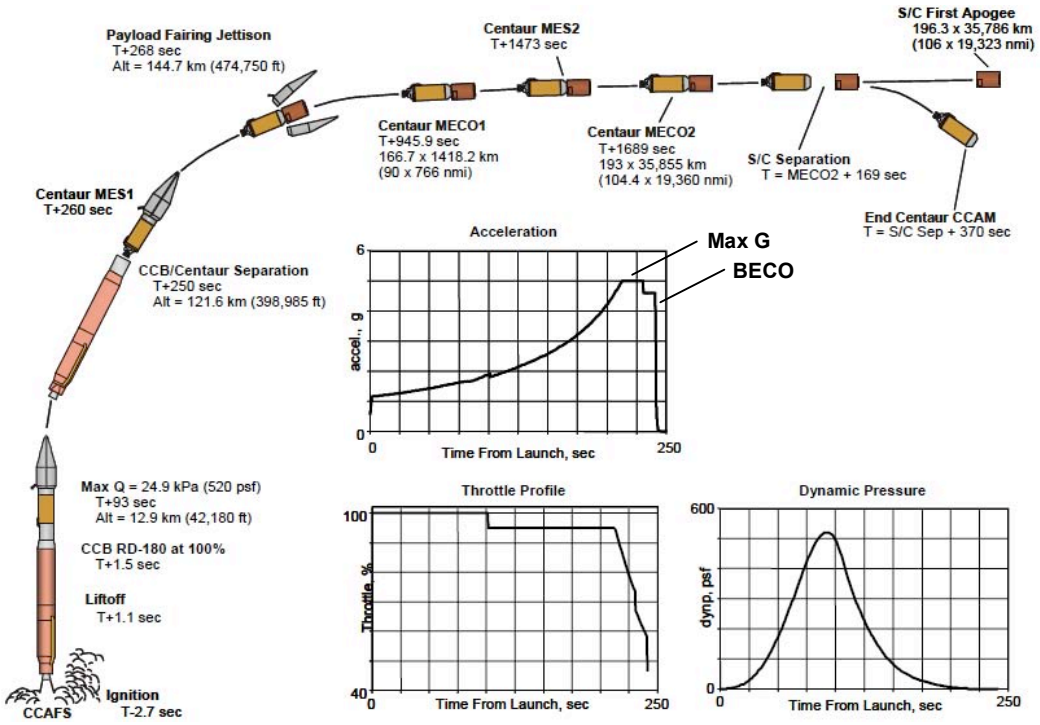

Fig 3. Typical Atlas V 401 standard short coast geosynchronous transfer orbit ascent profile [1].

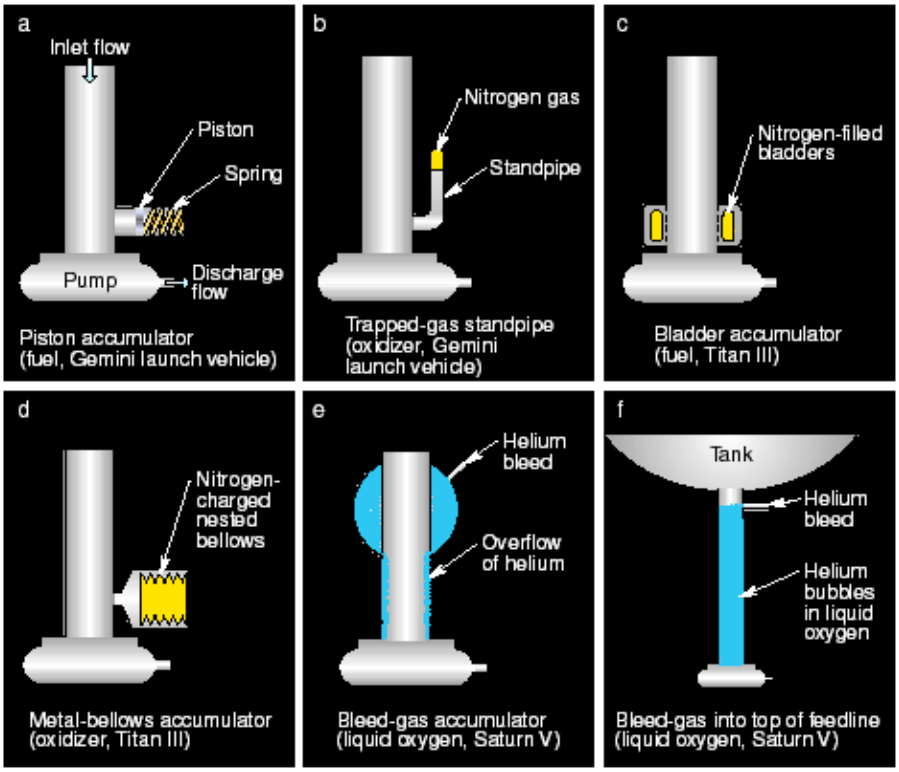

Fig 4. Schematics of accumulators that successfully suppressed pogo on various vehicles [2].

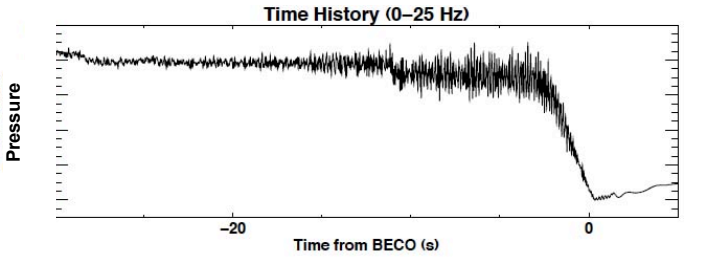

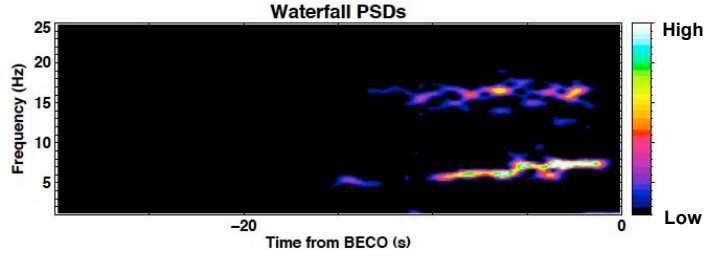

a) Pogo accumulator pressure.

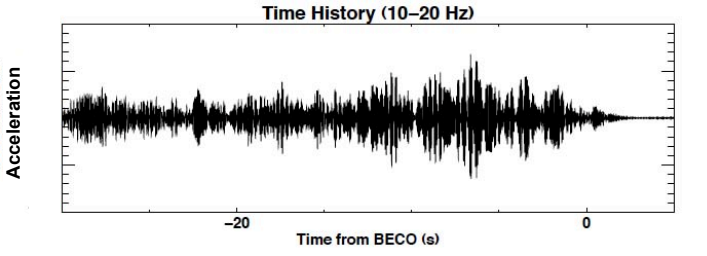

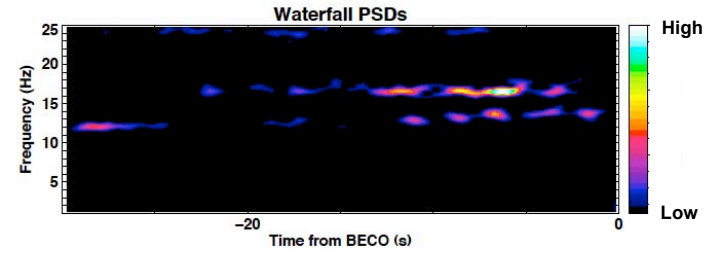

b) LO_2 feedline axial acceleration.

Fig 5. Measurements for an Atlas V flight and corresponding power spectral density.

The Atlas V altitude is exo-atmospheric at Max G, such that RD-180 engine thrust and low-frequency engine gimbaling are the only external forces that act on the vehicle. Atlas V responses due to oscillatory thrust are computed using structural models, subjected to a family of boost engine thrust oscillation (BETO) forcing functions. Preflight response predictions are based on statistics, computed for the family of BETO cases.

Because assessments of structural integrity require that response predictions envelop flight experience, the analysis must account for the engine-induced oscillations as well as any interactions between the structure and propellants.

In launch vehicle structural models, the propellants in feedlines and tanks are sometimes fixed to the launch vehicle hardware. That is, propellants are modeled as lumped masses that are rigidly attached to nodes of the structural model. This assumption precludes relative motion between liquid propellants and the ducts through which they flow. Interactions between liquid propellants and launch vehicle structure, consequently, are ignored.

Figure 5 shows bandpass-filtered time histories and waterfall displays of power spectral density for pogo accumulator pressure and LO_2 feedline acceleration.[1] It is evident that the 15-20 Hz oscillations in these measurements are related, and that they maximize just prior to BECO, during venting of the pogo accumulator.

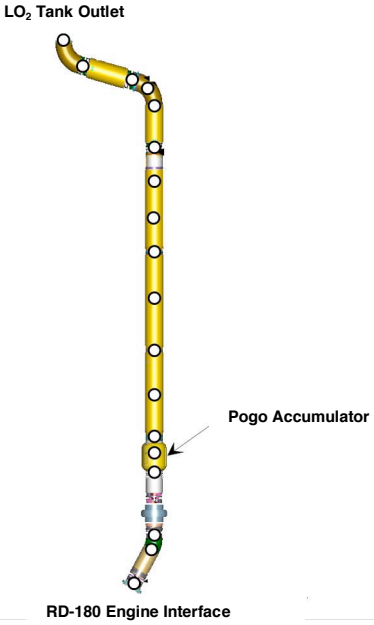

Fig 6. Fluid model. White dots represent nodes.

FLUID-STRUCTURE INTERACTION MODEL

Modeling Assumptions

The Max G FSI methodology development used structural models with LO_2 fixed to the feedline walls, in concert with equations for the interaction of liquid propellants and structure in rocket systems [4]. In other words, it was assumed that the modes from these models of the launch vehicle-spacecraft structure are a reasonable approximation of the structural characteristics of the actual system, and that the interactions of structural responses with fluid pressure and flow can be accounted for using the relationships in Ref. 4. This approach obviated the creation of structural models with indepen-

[1]Throughout this paper, figure scales are not shown because they may reveal company-proprietary information.

dent propellant motion and, thus, expedited the development of the methodology.

The equations in Ref. 4 are commonly used to assess linear stability with respect to the pogo phenomenon. An eigen analysis is conducted to establish the frequency and damping values for the closed-loop propulsion-structure system, where negative damping values indicate pogo instability [3,4].

The equations for propulsion-structure interaction can also be used to compute time histories of the propulsion and structure responses, provided that the closed-loop system is linearly stable. A time-domain analysis of the Max G phenomenon, therefore, was conducted using the equations in Ref. 4, after confirmation that the fluid-structure interaction yields a stable system.

The domain of the analysis was restricted to the LO_2 feedline. That is, representation of the fluid and structure extended from the tank outlet to the interface with the RD-180 engine. Although only structural data for the LO_2 feedline were required input, structural responses elsewhere on the launch vehicle-spacecraft system were readily computed, based on modal responses from the FSI analysis.

Fluid Model

The LO_2 feedline is shown in Fig. 6. Nodes of the fluid model are superimposed in the figure.

The fluid model included the tank outlet, gimbal elements, compressible duct elements, and the accumulator. For each of these elements, Ref. 4 provides relationships between structural response, fluid pressure, and fluid flow. There are 25 interfaces in the fluid model, each with its own pressure and flow value. Hence, the fluid model has 50 degrees of freedom.

Parameters that describe the fluid elements include density, inertance, flow rate, linear resistance, stiffness, head vectors, interface normal vectors, and correlation with specific grids of the structural model [4]. These parameters are considered constant, except for flow rate and linear resistance, which vary with analysis time.

Details of the LO_2 feedline hardware are company proprietary information, such that the fluid element assemblage cannot be elaborated beyond Fig. 6 and the preceding paragraphs.

Structural Model

In the structural model, the LO_2 feedline is composed of beam elements. This beam model is coupled to models of the other launch vehicle and spacecraft components to generate a system dynamic model. Eigen analysis of this dynamic model yields natural frequencies and mode shapes.

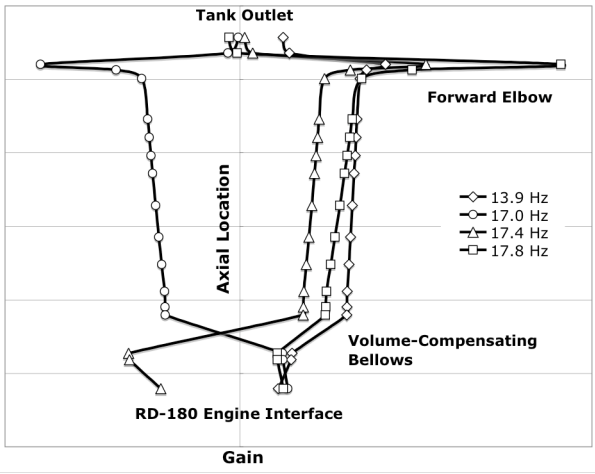

Fig 7. Axial gains of structural modes for an Atlas V mission.

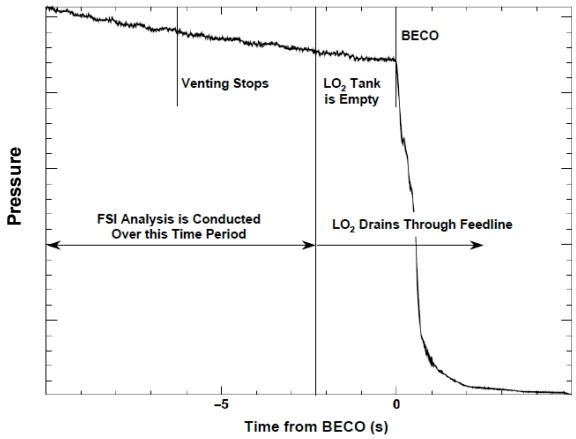

Fig 8. Atlas V events and FSI analysis period.

Only the gains of the LO_2 feedline, corresponding to the coupled system modes, are required inputs for the FSI analysis. However, the responses at all positions in the coupled system dynamic model can be computed using time histories of the generalized structural coordinates from the FSI analysis.

Structural modes in the range 10-20 Hz were selected for the FSI analysis. Because the system model accounts for the dynamic characteristics of the spacecraft, and because the Atlas V vehicle launches a variety of spacecraft, the modal properties for the LO_2 feedline depend on the Atlas V mission of interest. The FSI analysis results, consequently, depend on the structural characteristics of the mission being analyzed.

Axial gains of key structural modes for an Atlas V mission are shown in Fig. 7.[2] Note that there is a sharp increase in axial gain at the forward elbow of the feedline. It will be shown that LO_2 pressure acting at this elbow tends to excite the modes shown.

Analysis Period

Figure 8 shows the timing of Atlas V events and the period over which the FSI analysis is conducted. The analysis initiates at BECO-10s.

The propellant drains through the tank and the feedline as BECO approaches. The LO_2 tank is completely empty, but the feedline is completely full, shortly before BECO. This time point represents the end of the FSI analysis period. Venting of the pogo accumulator stops at roughly the midpoint of the FSI analysis period.

Pogo Accumulator Venting

Figure 9 shows the variation in pogo accumulator stiffness and linear resistance over the FSI analysis period.

Gas within the pogo accumulator provides compliance, such that the feedline fundamental hydraulic mode has a natural frequency that remains well below the critical axial modes of the structure. When gas is vented from the acccumulator, prior to BECO, the compliance decreases (stiffness increases), such that the natural frequency of the fundamental hydraulic mode increases.

The linear resistance of LO_2 flow through the accumulator communication holes also changes during the venting process. The resistance increases due to quasi-steady flow into the accumulator, but then decreases sharply when venting ceases.

Forcing Functions

Five forcing functions were applied to the fluid-structure interaction model: 1) boost engine thrust oscillations (BETO), 2) broadband feedline noise induced by the venting process, 3) nonoscillatory forces associated with draining of the LO_2 tank prior to BECO, 4) nonoscillatory LO_2 flow into the accumulator during the venting process, and 5) oscillatory LO_2 flow into and out of the accumulator communication holes, due to structural vibration.

Flight-derived BETO forcing functions were applied during FSI analyses aimed at reconstructing flight data. However, for preflight prediction of responses, a family of BETO forcing functions were applied to conventional structural models. The BETO results were combined statistically with those from FSI analyses conducted with the forcing functions numbered 2-5 above.

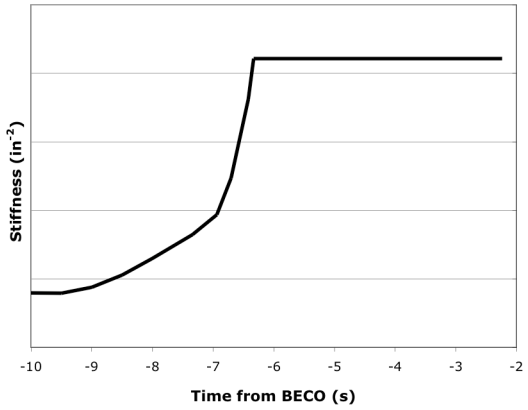

a) Pogo accumulator stiffness.

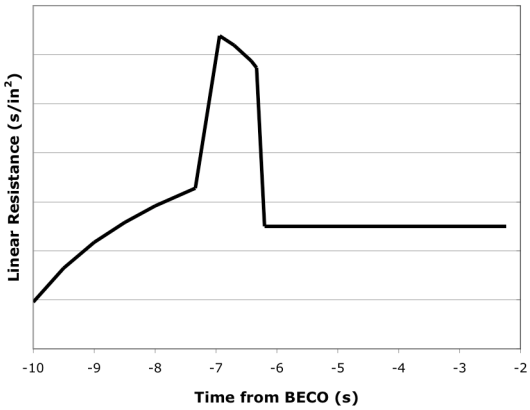

b) Pogo accumulator linear resistance.

Fig 9. Variation in pogo accumulator properties during FSI analysis period.

Current FSI development efforts have relied upon developing an oscillatory LO_2 weight displacement forcing function tuned to a specific frequency that is based upon flight data and the model's frequency response function. Since the frequency cannot be determined *a priori*, a family of twenty-one narrow-band weight displacement forcing functions was developed to be used for FSI preflight predictions.

The shock response spectra (SRS) of accumulator weight displacements from previous flights provided the basis for establishing the frequency band and amplitude of these forcing functions, as shown in Fig. 10a. A power spectral density (PSD) input, defined over 14-17.5 Hz, that would, on average, yield a maximum response equal

[2] Lateral gains are also included in the FSI analysis but, for brevity, are not shown here.

to A_{max} was calculated using Mile's equation and the Rayleigh distribution of peaks [5].

The resulting root-mean-square value was then used to scale 21 narrow-band signals that were developed by band-pass filtering of broad-band Gaussian signals. The response spectra of these forcing functions were calculated and plotted with their mean and statistical enclosure level in Fig. 10b. The ratio of the statistical bound and the mean value is approximately 1.5.

NUMERICAL ANALYSIS

Formulation of the FSI phenomenon by pogo-type modeling leads to the following time-varying second order linear differential equation

$$\mathbf{M}(t)\ddot{\mathbf{x}}(t)+\mathbf{C}(t)\dot{\mathbf{x}}(t)+\mathbf{K}(t)\mathbf{x}(t)=\mathbf{f}(t) \qquad (1)$$

where, $\mathbf{x}(t)$, is the state vector representing the pressures, weight displacements, and generalized structural displacements

$$\mathbf{x}(t)=\left\{p_1(t),\ldots,p_{25}(t),\ w_1(t),\ldots,w_{25}(t),\ q_1(t),\ldots,q_m(t)\right\}^T \quad (2)$$

and **f**(*t*) encompasses the five forcing functions discussed previously.

Numerical integration via the 4th order Runge-Kutta method (RK-4) was chosen because 1) it is efficient in terms of step size and accuracy, and 2) it is the numerical integrator used in other dynamic analyses, which permitted convenient validation of its implementation in the FSI program.

RK-4 involves recasting Eq. (1) to a first order system that requires inversion of the "mass matrix", **M**(*t*). However, as is typical with pogo-type modeling, **M**(*t*) is rank deficient, and therefore, cannot be inverted directly.

To investigate the source of these singularities, matrix topologies that indicate the non-zero matrix elements for all matrices in Eq. (1) were determined and plotted. Fig. 11 displays the topologies of both the open-loop and closed-loop matrix **M**(*t*).

Examination of these topologies reveal that the singularities are due to zero rows and columns that occur in both **M**(*t*) and **C**(*t*). The zero rows are associated with constraints that equate the outlet and inlet pressures and flows of adjoining fluid elements. Hence, these equations and redundant state variables were easily removed by Guyan reduction.

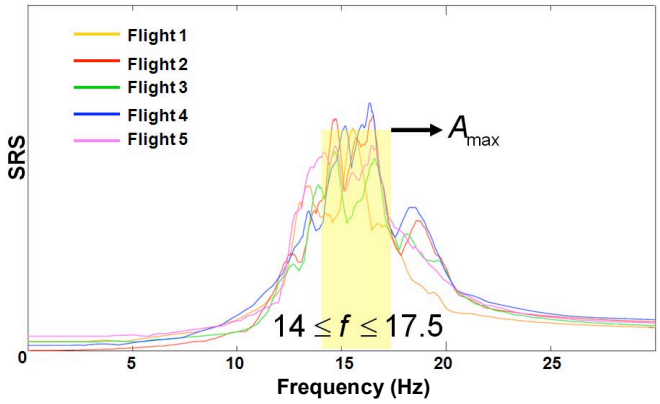

a) SRS from five Atlas V flights.

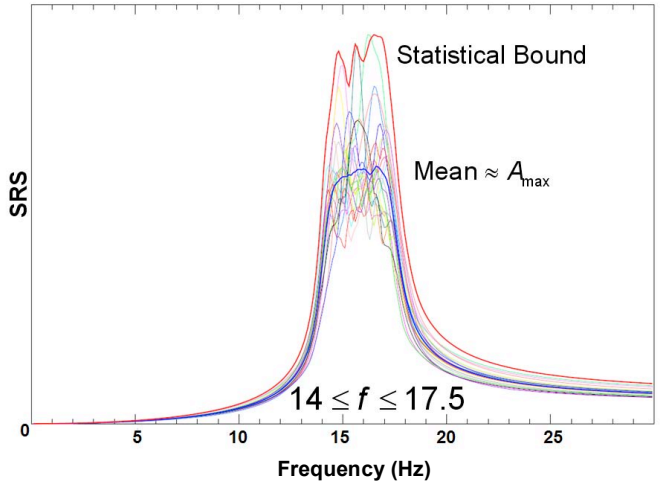

b) SRS from 21 narrow-band forcing functions with mean and statistical bound.

Fig 10. Weight displacement SRS.

The zero columns that appear in the resulting reduced **M**(*t*) and **C**(*t*) matrices correspond to state variables whose derivatives do not appear in the reduced equations. Therefore, these variables can be removed by expressing them as linear combinations of the remaining variables and their derivatives. This reduction was performed at each time point resulting in a reduced mass matrix that was invertible. As a final check, the eigenvalues of both the unreduced and reduced systems were computed and shown to be identical.

The reduced set of equations were numerically integrated using RK-4. Several integration step sizes were used to demonstrate convergence. The responses were expanded to the complete set of state variables using the transformations that were applied during the reduction process. Finally, the acceleration transformation

matrix was applied to recover physical accelerations along the vehicle.

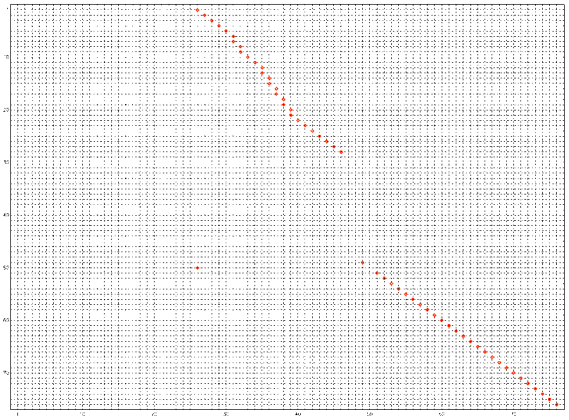

a) Topology of open-loop **M**(*t*) matrix.

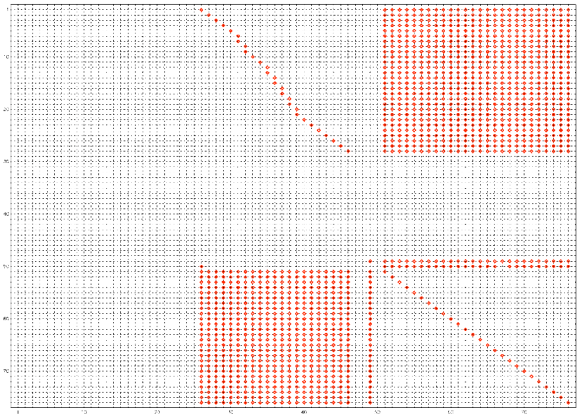

b) Topology of closed-loop **M**(*t*) matrix.

Fig 11. Topology of **M**(*t*) that indicates the non-zero elements in red.

RESULTS

Open-Loop Hydraulic Modes

The natural frequencies and damping values of the first three hydraulic modes are shown in Fig. 12. The frequency increase during venting is caused by the rise in pogo accumulator stiffness (see Fig. 9a). The damping increase during venting is caused by resistance during quasi-steady LO_2 inflow to the accumulator (see Fig. 9b).

The symbols in Fig. 12 indicate the times at which FSI models were assembled. The term "long column" refers to modes dominated by pressure and flow forward of the pogo accumulator. The term "short column" refers to modes dominated by pressure and flow aft of the pogo accumulator.

Pressure and weight displacement for the first three open-loop hydraulic modes are shown in Fig. 13.[3] The mode shapes at the beginning and end of the FSI analysis period are different due to changes in the fluid element properties.

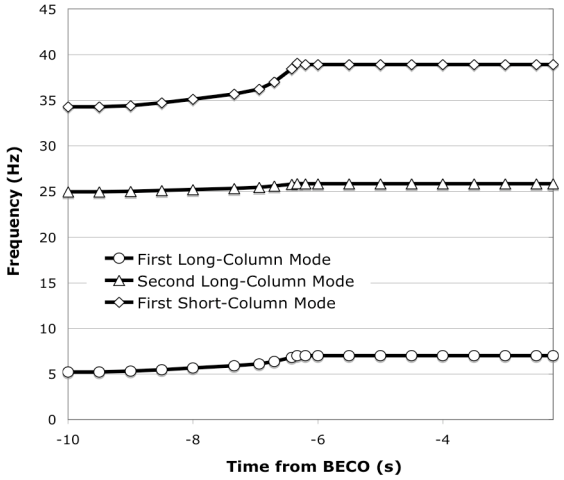

a) Natural frequencies of open-loop hydraulic modes.

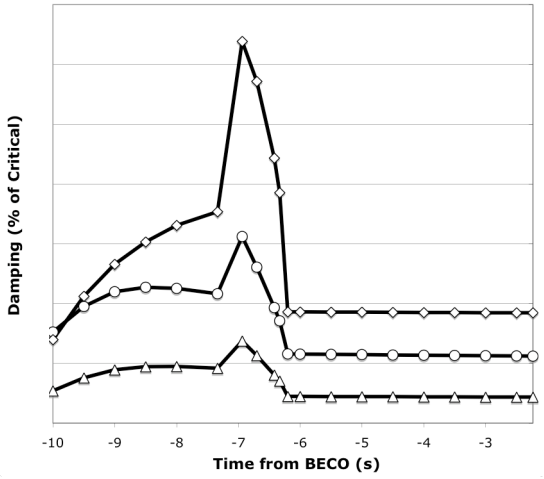

b) Damping values of open-loop hydraulic modes.

Fig 12. Frequencies and damping values for first three hydraulic modes, as function of analysis time.

Flight Reconstruction

The lateral acceleration at the spacecraft interface for an Atlas V mission is compared in Fig. 14 with results from the BETO-only analysis and from the closed-loop FSI analysis. The thrust oscillation forcing function, which is applied in both the BETO and FSI analyses, was derived from engine pressure flight data.

[3] The mode shapes are complex valued; for brevity, only the real parts are plotted.

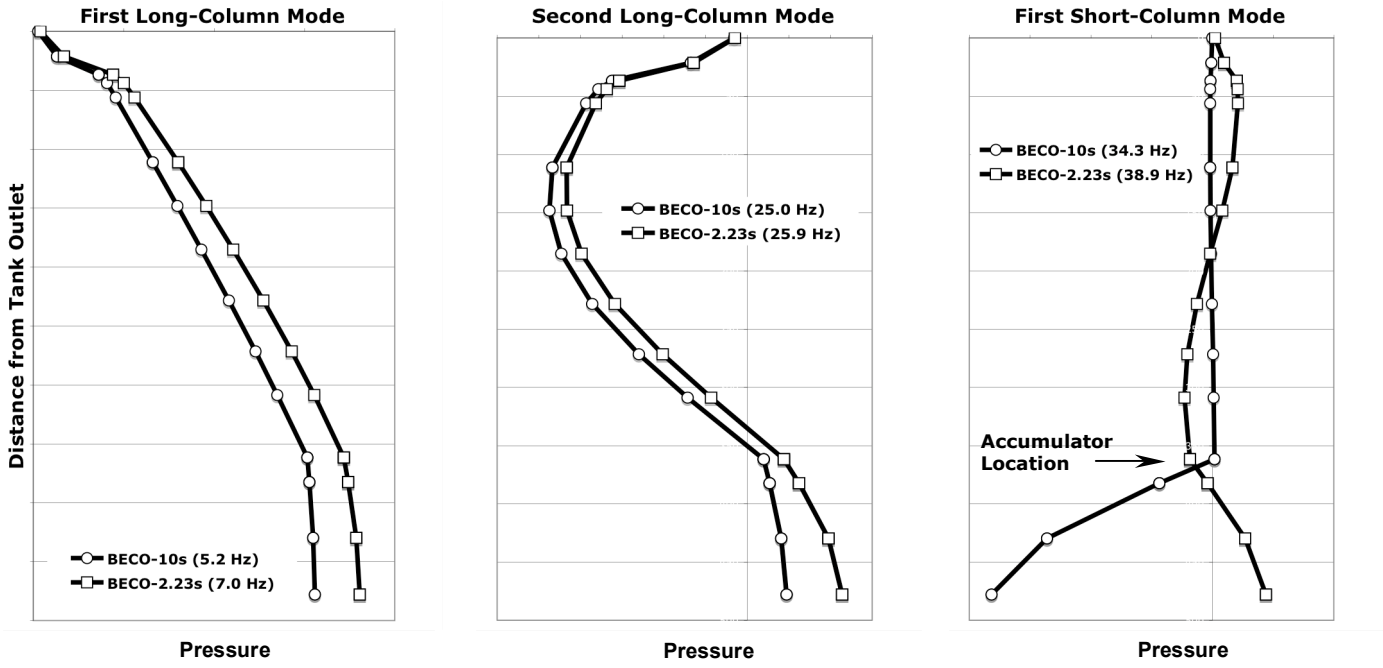

a) Pressure mode shape.

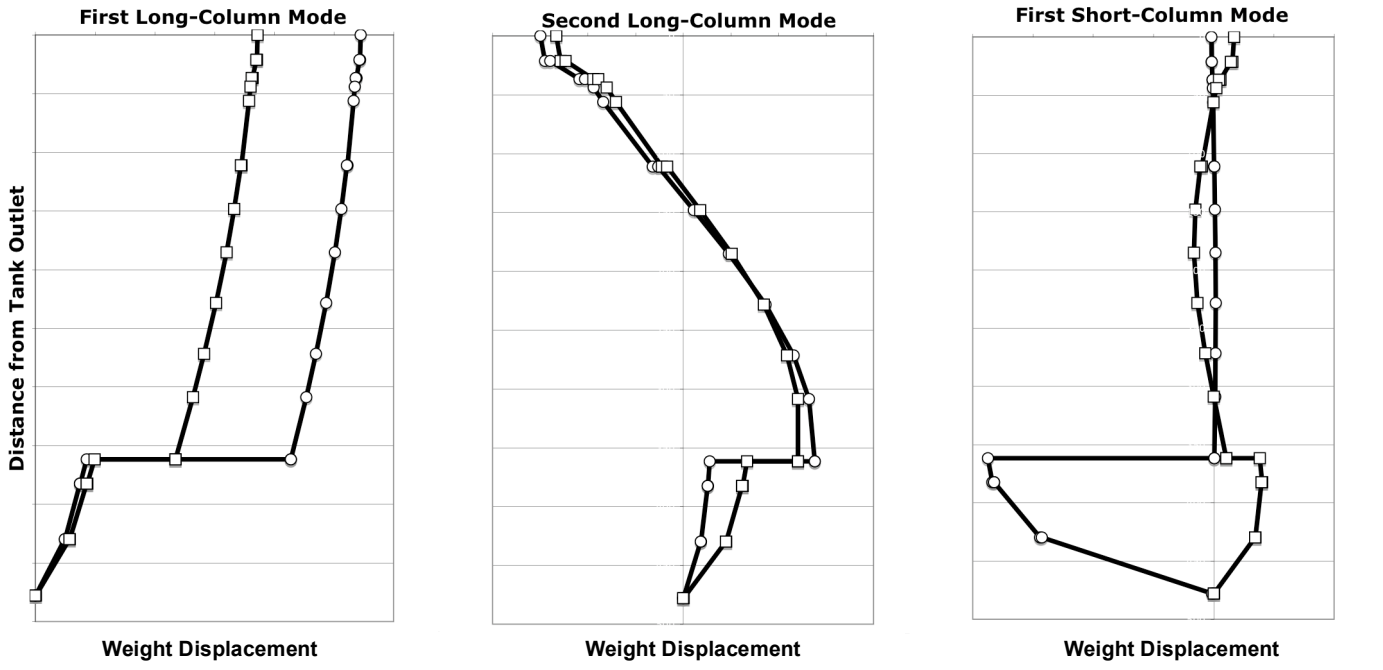

b) Weight displacement mode shape.

Fig 13. Open-loop hydraulic mode shapes from FSI analysis. Real parts of complex pressure and weight displacement are shown.

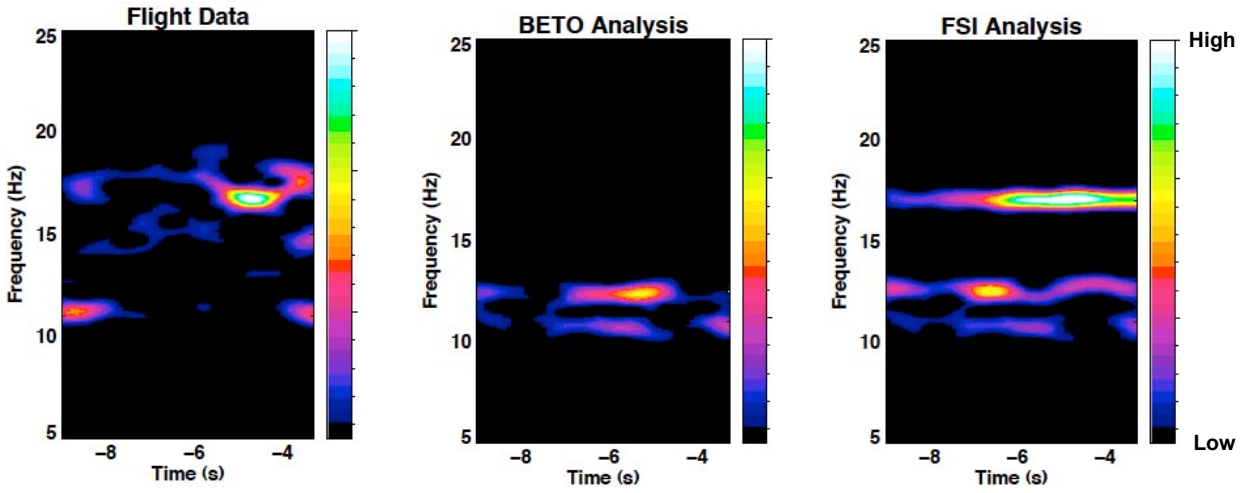

a) Waterfall plots of power spectral density.

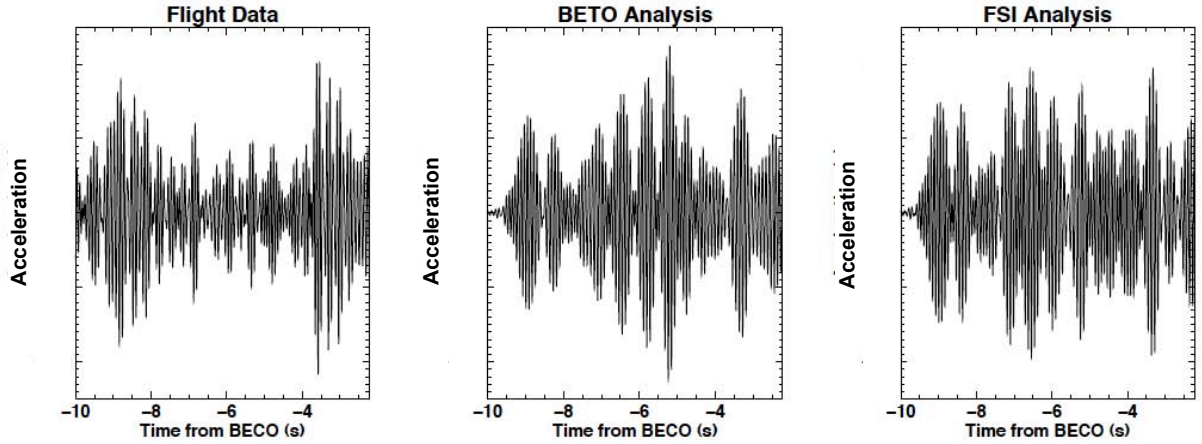

b) 10-15 Hz bandpass filtered responses.

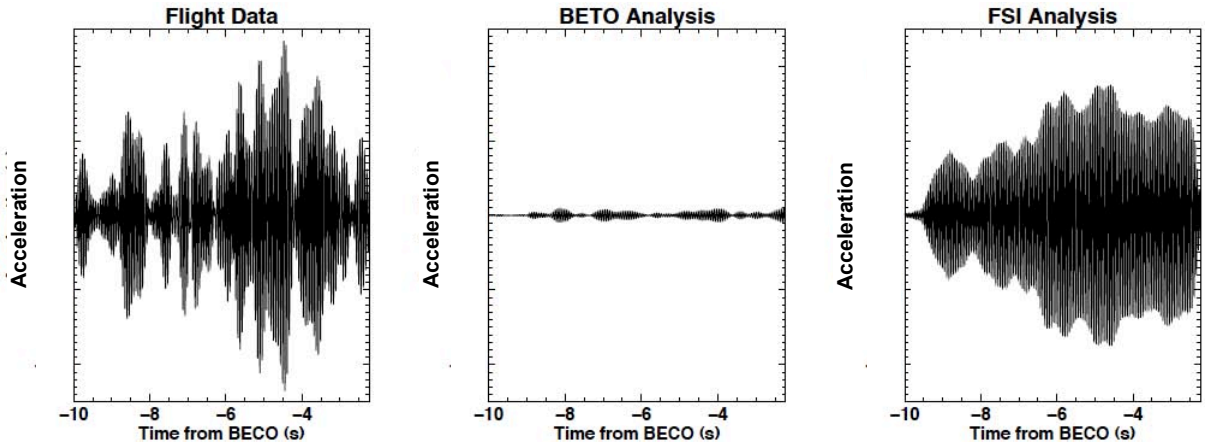

c) 15-20 Hz bandpass filtered responses.

Fig 14. Comparison of spacecraft interface lateral acceleration measurement with results from traditional BETO analysis and from closed-loop FSI analysis. Both analyses use thrust oscillation forcing function derived from engine data.

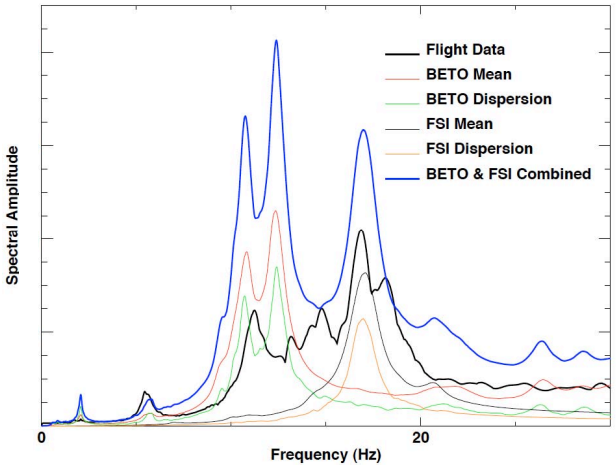

Fig 15. BETO and FSI statistical spectral amplitudes for spacecraft interface lateral response at Max G.

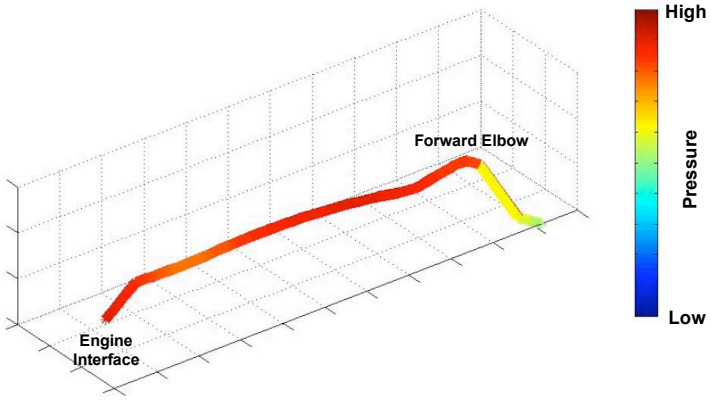

a) BECO-5.02s.

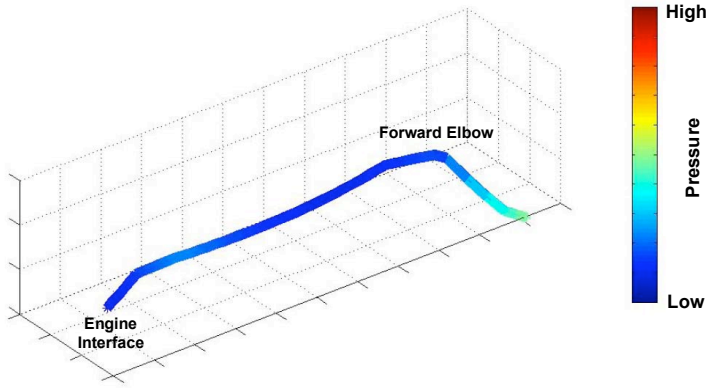

b) BECO-4.99s.

Fig 16. FSI analysis pressures and deformed LO_2 feedline.

Figure 14a shows waterfall plots of power spectral density. Note that the FSI analysis yields a 17-Hz response with the same time of occurrence as flight data. The BETO-only analysis does not yield this 17-Hz response because fluid-structure interaction is ignored.

Figures 14b and 14c show bandpass-filtered acceleration time histories. It is evident that the 10-15 Hz responses are caused by boost engine thrust oscillations. The BETO-only analysis reproduces the response amplitude in this frequency range.

The 15-20 Hz responses are caused by fluid-structure interaction. The BETO-only analysis underpredicts the amplitude in this frequency range. However, the closed-loop FSI response approximates flight data.

The FSI analysis yields acceptable agreement with flight response amplitudes and trends, but refinements to the accumulator venting model, feedline noise forcing function, and launch vehicle structural model are being pursued. The goals of the analysis refinement are to improve correlation with flight data, to expand our understanding of the root cause of the Max G phenomenon, and to identify mitigation strategies.

Statistical Preflight Prediction

The forcing functions that a mission will experience during flight are not known with accuracy prior to flight. In coupled loads analysis methodology, it is common to generate a family of representative forcing functions. Statistics are then computed using the responses that result when the family of forcing functions is applied to the mission-specific coupled system model.

A family of BETO forcing functions is applied to conventional structural models, and statistics are computed using the resulting responses. A family of accumulator weight displacement forcing functions is also constructed. This family is applied in the FSI analysis, without BETO forces. The BETO and FSI responses are then combined to yield a statistical bound. The statistical bound is then evaluated, before flight, to ensure that the mission has adequate structural margin.

The statistical spectral amplitudes of BETO and FSI responses are shown in Fig. 15 for an Atlas V mission. The combined response (blue curve) is given by the sum of the BETO and FSI means plus the root-sum-square of the BETO and FSI dispersions. This combination should envelop the spectral amplitude from flight data (black curve), in order to be considered an acceptable response prediction. Figure 15 shows that the combination does indeed bound flight data, whereas predictions based solely on the engine thrust oscillation forcing functions do not.

Correlation Between Pressure and Displacement

Oscillatory feedline pressure and structural displacement from the closed-loop FSI analysis are shown in Fig. 16 for time points separated by one-half of one 17-Hz vibration cycle. Figure 16a shows the feedline deformation at maximum pressure amplitude, while Fig. 16b shows the deformation 0.03s later, at the minimum pressure value.

Note that the forward elbow stretches during maximum pressure, and contracts under minimum pressure. In other words, pressure applied to the projected area at the forward elbow excites the feedline, consistent with the structural mode shapes shown in Fig. 7.

CONCLUSIONS

During some periods of Atlas V flight, structural responses of the coupled system can interact with fluid responses of the LO_2 feedline. Venting of the pogo accumulator, which occurs prior to cutoff of the boost engine, excites the fluid-structure system and changes the stiffness and damping characteristics of the feedline hydraulic modes. For the Atlas V launch vehicle, responses tend to increase at cessation of pogo accumulator venting. Structural models that rigidly attach the LO_2 propellant to the feedline walls underpredict Atlas V flight responses at Max G. Incorporation of FSI in response analyses eliminates this deficiency.

ACKNOWLEDGMENT

Wing K. Yeung implemented changes to the pogo stability code required for the FSI analysis. Earl J. Parker created animations of the FSI results. Herand Bedrossian, Brett E. Soltz and Filiberto Urias generated the coupled system dynamic model for the mission analyzed in this paper. Trinh T. Nguyen created the pogo accumulator venting model. John W. Murdock evaluated the accumulator venting noise level. Finally, S. Rubin provided guidance regarding incorporation of the venting model in the FSI analysis. The contributions of these colleagues are gratefully acknowledged.

REFERENCES

[1] Sponnick, J., 2007, "Atlas Launch System Mission Planner's Guide," CLSB-0409-1109, Rev. 10a, Lockheed Martin Corp., Denver, CO.

[2] Dotson, K., Winter 2003/2004, "Mitigating Pogo on Liquid-Fueled Rockets," Crosslink, 5(1), The Aerospace Corporation, El Segundo, CA, pp. 26-29.

[3] Rubin, S., 1970, "Space Vehicle Design Criteria (Structures): Prevention of Coupled Structure-Propulsion Instability (POGO)," NASA SP-8055.

[4] Oppenheim, B. W., and Rubin, S., 1993, "Advanced Pogo Stability Analysis for Liquid Rockets," Journal of Spacecraft and Rockets, Vol. 30(3), pp. 360-373.

[5] DiMaggio, S. J., Sako, B. H., and Rubin, S., 2003, "Analysis of Nonstationary Vibroacoustic Flight Data Using a Damage-Potential Basis," Journal of Spacecraft and Rockets, Vol. 40(5), pp. 682-689.